Molecular Crystals and Liquid Crystals
Publication details, including instructions for authors and subscription information:
http://www.tandfonline.com/loi/gmcl16

Computer Simulation of Molecular Dynamics of Anisotropic Fluids

Didier Decoster [a] , EugÈNe Constant [a] & Monique Constant [b]

[a] Centre Hyperfréquences et Semiconducteurs (LA CNRS 287), Université des Sciences et Techniques de Lille, Bât P3 59655 Villeneuve, D'ascq, Cedex, France

[b] Laboratoire de Spectrochimie Infrarouge et Raman (LP CNRS 2641), Université des Sciences et Techniques de Lille, Bât C5 59655 Villeneuve, D'ascq, Cedex, France

Version of record first published: 17 Oct 2011.

Mol. Cryst. Liq. Cryst., 1983, vol. 97, pp. 263–276
0026-8941/83/9704–0263/$18.50/0

Computer Simulation of Molecular Dynamics of Anisotropic Fluids†

DIDIER DECOSTER and EUGÈNE CONSTANT

Centre Hyperfréquences et Semiconducteurs (LA CNRS 287) Université des Sciences et Techniques de Lille, Bât P3 59655 Villeneuve D'ascq Cedex, France

and

MONIQUE CONSTANT

Laboratoire de Spectrochimie Infrarouge et Raman (LP CNRS 2641) Université des Sciences et Techniques de Lille, Bât C5 59655 Villeneuve D'ascq Cedex, France

(Received January 24, 1983)

Molecular dynamics calculations have been performed for fluid systems containing ellipsoidal particles which interact pair-wise with a modified Lennard-Jones potential. Assuming molecular parameters close to those of the CB7 compound, we have calculated both static and dynamic properties such as the internal energy, the entropy and specific heat changes at T_{NI}, the compressibility factor, the temperature dependence of the orientational order parameters, the reorientational angular momentum and velocity time-dependent self-correlation functions, and the diffusion coefficients in both the nematic and isotropic phases. The thermodynamical data show a transition between isotropic and nematic phases and the results obtained are in qualitative agreement with the experimental data. The influence of a decenterd dipole along the molecular axis has been studied and partially bilayered smectic phases have been obtained.

INTRODUCTION

By "computer experiments" one can attempt to bridge the gap between the microscopic (molecular) and macroscopic (phenomenological) aspects of liquid crystal physics.[1–4] Our aim is to use this method to study the effect of molecular structure on the physical properties and on the stability of mesophases by testing various kinds of interaction. In this paper, we focus attention on uniaxial systems.

†Presented at the Ninth International Liquid Crystal Conference, Bangalore, December 6–10, 1982.

NUMERICAL PROCEDURE

The molecular dynamics technique consists of studying the movement of N particles in a parallelepipedic box (volume V); the particles interact[5] pairwise with a two-body potential V_{ij}. To do this, we solve the coupled Euler-Newton equations of motion using an algorithm developed by Verlet[6] and Quentrec[7] and we deduce, at each step of the calculation, the position, orientation, velocity and angular momentum of each particle. Then, these values are recorded on a magnetic tape, and the macroscopic quantities, which define the system involved, are deduced by performing statistical averages.

Because of technical limits, which are in fact time-computer limits, the number of particles is very small and, in order to reduce the surface effects of the box, we employ the common artefact of periodic boundaries.[5] In the same way, since for liquid crystals, the number of atoms in each molecule can be higher than 30, the interaction cannot be an atom-atom interaction. Consequently, we have chosen a two-body potential which depends only upon the relative position and orientation of the particles. Moreover, in a first approximation, we have neglected the effect of the rotation of the particles around their symmetry axis. As a consequence, V_{ij} has cylindrical symmetry, and we perform our calculation with five degrees of freedom (three translational and two rotational).

FIRST APPLICATION OF THE METHOD

We consider ellipsoidal particles, with major and minor axes $\sigma_\parallel$ and $\sigma_\perp$ respectively, which interact pairwise with a modified Lennard-Jones potential previously proposed by Berne:[1,8]

$$V_{ij} = 4\varepsilon[(\sigma/r_{ij})^{12} - (\sigma/r_{ij})^6] \tag{1}$$

where

$$\varepsilon(\mathbf{u}_i, \mathbf{u}_j) = \varepsilon_0[1 - \chi^2(\mathbf{u}_i \cdot \mathbf{u}_j)^2]^{-1/2} \tag{2}$$

$$\sigma(\mathbf{u}_i, \mathbf{u}_j, \mathbf{r}_{ij}) = \sigma_\perp \cdot \left\{1 - \frac{1}{2}\chi\left[\frac{\left(\frac{\mathbf{r}_{ij}\cdot\mathbf{u}_i}{r_{ij}} + \frac{\mathbf{r}_{ij}\cdot\mathbf{u}_j}{r_{ij}}\right)^2}{1 + \chi(\mathbf{u}_i\cdot\mathbf{u}_j)} + \frac{\left(\frac{\mathbf{r}_{ij}\cdot\mathbf{u}_i}{r_{ij}} - \frac{\mathbf{r}_{ij}\cdot\mathbf{u}_j}{r_{ij}}\right)^2}{1 - \chi(\mathbf{u}_i\cdot\mathbf{u}_j)}\right]\right\}^{-1/2} \tag{3}$$

$$\chi = \frac{(\sigma_\parallel/\sigma_\perp)^2 - 1}{(\sigma_\parallel/\sigma_\perp)^2 + 1} \tag{4}$$

$\mathbf{u}_i$ and $\mathbf{u}_j$ are the orientation vectors of the two particles; $\mathbf{r}_{ij}$ is a vector joining the two centers; it has magnitude r_{ij}, the distance between two centers. In Figure 1, we represent the two-body potential for different orientations of the particles. It appears that the interactions are mainly governed by steric effects. The parameters of the model are given in Table I; they have been chosen to be close to those for 7CB (4′-n-heptyl-4-cyanobiphenyl). At the start of the calculation, the molecules lie along the Z axis, which defines the optical axis.[4] During the first 30 ps, the system runs and reaches its equilibrium state. Then the static and dynamic properties can be studied. All the systems obtained obey the conservation principles (energy, momentum) and the equipartition theorem.

Static properties

For all the temperatures investigated, the translational order parameter

$$S_t = \langle \cos \mathbf{k} \cdot \mathbf{r} \rangle \tag{5}$$

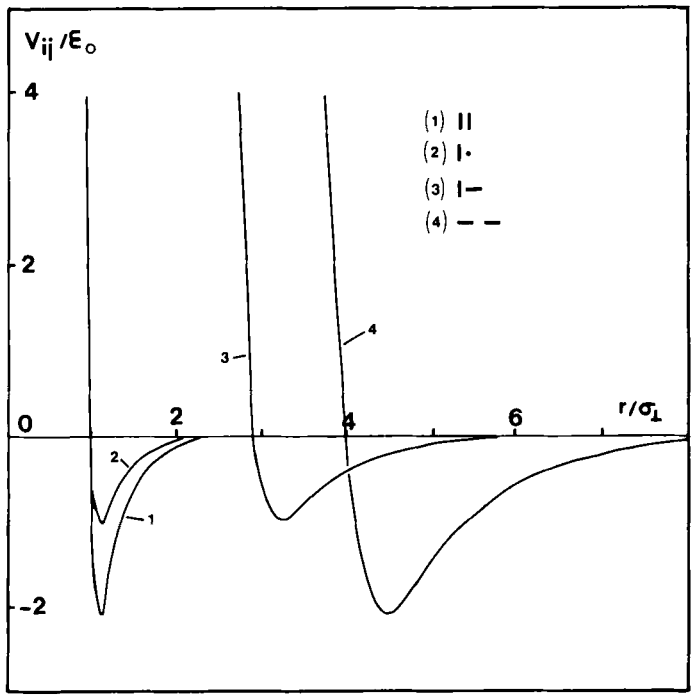

FIGURE 1 Two body potential for different orientations of the particles; $\sigma_{\parallel} = 17.9$ Å, $\sigma_{\perp} = 4.5$ Å.

TABLE I

Parameters of the model; the case of ellipsoidal particles: the mass m is the mass of the compound 7CB;[9] the transverse inertial moment I is calculated assuming an ellipsoid of uniform mass m; $\sigma_\parallel$ and $\sigma_\perp$ are deduced from X-ray data;[10] N/V is the density of the particle of the compound 7CB in the nematic state near the nematic-isotropic transition temperature;[11] k_B is the Boltzmann constant.

m (Kg)	I (Kg · m^2)	$\sigma_\parallel$ (Å)	$\sigma_\perp$ (Å)	ε_0/k_B (K)	N/V (m^{-3})	N
$4.61\ 10^{-25}$	$17.5\ 10^{-44}$	17.9	4.5	53.4	$2.16\ 10^{27}$	27

where the brackets $\langle\ \rangle$ denote an ensemble and time average and $\mathbf{k}$ is the smallest vector of the reciprocal lattice, has been found equal to zero within statistical errors (#2%). Consequently the simulated systems can be likened to fluids. The variations in the internal energy (kinetic + potential) per particle

$$U_i = \frac{1}{2}m\langle v^2\rangle + \frac{1}{2}\mathrm{I}\langle\omega^2\rangle + \frac{1}{N}\left\langle \sum_{j<i=1}^{N} V_{ji} \right\rangle \tag{6}$$

(where v and ω are the translational and rotational velocities) plotted against temperature are given in Figure 2-1. The two slopes (specific heat) and the small step in energy suggest an anisotropic-isotropic fluid transition. This is confirmed by the variations in the orientational order parameters with temperature (Figure 2-2). In the isotropic phase, the value of $\langle P_2\rangle$ does not exactly fall to zero, because the edges of the box are lower than the coherence length. In Table II, we compare the results obtained from the simulation at the nematic-isotropic transition with those obtained from experiments. The agreement is rather good, except for the pressure P and $\langle P_4\rangle$.

We have also studied the short range angular correlations using the relation:

$$\langle P_{2l}(r)\rangle = \frac{1}{2}\langle 3\cos^2\theta_{ij}(r) - 1\rangle \tag{7}$$

where θ_{ij} is the angle between the axis of the i^{th} and j^{th} particles, separated by a distance r (in fact, the averages are performed on the surrounding particles of an i^{th} particle contained in an ellipsoidal skin with a minor axis $2r$ and major axis $2r \cdot (\sigma_\parallel/\sigma_\perp)$ parallel to the optical axis). In the nematic state (Figure 3-1), the angular correlations are very strong and remain in the isotropic state, according to the Landau-de Gennes theory[14] and many experiments.[13,15] The center of gravity distribution around one particle is given by

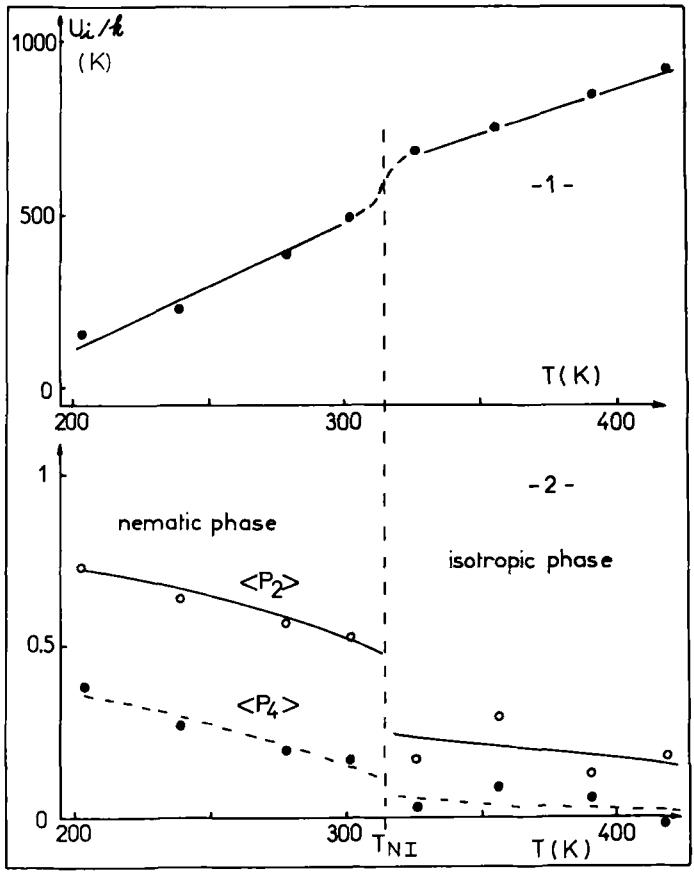

FIGURE 2-1 Total energy per molecule vs the temperature. For $T < T_{NI}$, the slope which represents the specific heat C_v is about 3.5 k_B; for $T > T_{NI}$, the slope is close to 2.5 k_B.
FIGURE 2-2 Orientational order parameters vs the temperature: $\langle P_2 \rangle = \frac{1}{2}[3\langle \cos^2 \theta \rangle - 1]$; $\langle P_4 \rangle = \frac{1}{8}[\langle 35 \cos^4 \theta \rangle - 30\langle \cos^2 \theta \rangle + 3]$. θ is the angle between the molecular axis and the optical axis.

$$G(r) = \frac{\langle \Delta N(r) \rangle}{\Delta V(r)} \frac{V}{N} \tag{8}$$

where ΔN is the number of particles in a small volume ΔV; r has the definition given in the relation in Eq. (7). It shows a liquid-like behavior in the isotropic and nematic states (Figure 3-2).

Dynamic properties

In Figure 4, we report the reorientational self-correlation functions (s.c.f.)

TABLE II

Comparison between the results obtained at the nematic-isotropic transition temperature T_{NI} from the simulation and from experiments. The entropy change ΔS at T_{NI} is equal to $\Delta U_i/k_B$. The pressure P is deduced from the virial theorem:

$$P = \frac{NkT}{V} + \frac{1}{3V}\left\langle \sum_{j<i=1}^{N} \mathbf{f}_{ji} \cdot \mathbf{r}_{ji} \right\rangle$$

where $\mathbf{f}_{ji}$ and $\mathbf{r}_{ji}$ are the force and the distance between te j^{th} and i^{th} particles.

$T = T_{NI}$	Measurements	Simulation
$\langle P_2 \rangle$	.42[12]	.48
$\langle P_4 \rangle$	−.06[12]	.09
ΔS	.24 k_B[13]	.3 k_B
PV/Nk_BT	.01	6.5

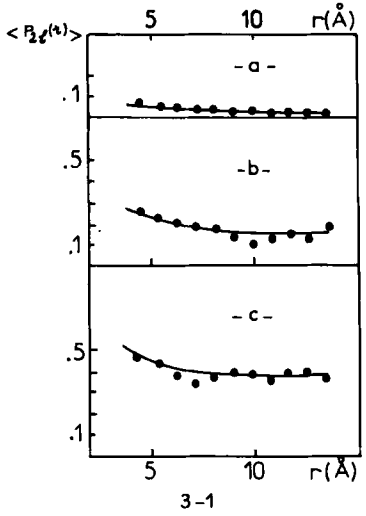

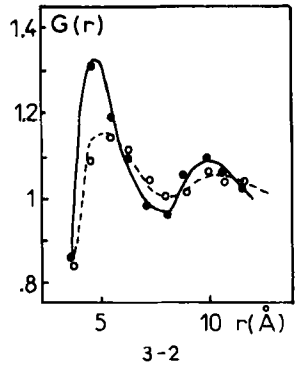

FIGURE 3-1 Short range angular correlations; (a) isotropic phase T = 392 K; (b) isotropic phase T = 326 K; (c) nematic phase T = 240 K.

FIGURE 3-2 Center of gravity distribution around one particle: (——) anisotropic phase T = 240 K; (---) isotropic phase T = 392 K.

$$\phi_{u_{\parallel'\perp}}(t) = \frac{\langle u_{\parallel'\perp}(0) u_{\parallel'\perp}(t) \rangle}{\langle u^2_{\parallel'\perp}(0) \rangle} \tag{9}$$

where $u_\parallel$ and $u_\perp$ are the components of a unit vector along the molecular axis, parallel and perpendicular to the optical axis. In the nematic state, the behavior of $\phi_{u_\parallel}(t)$ and $\phi_{u_\perp}(t)$ indicates rare end to end reorientations and a slow and diffusive motion around the director. In the isotropic phase,

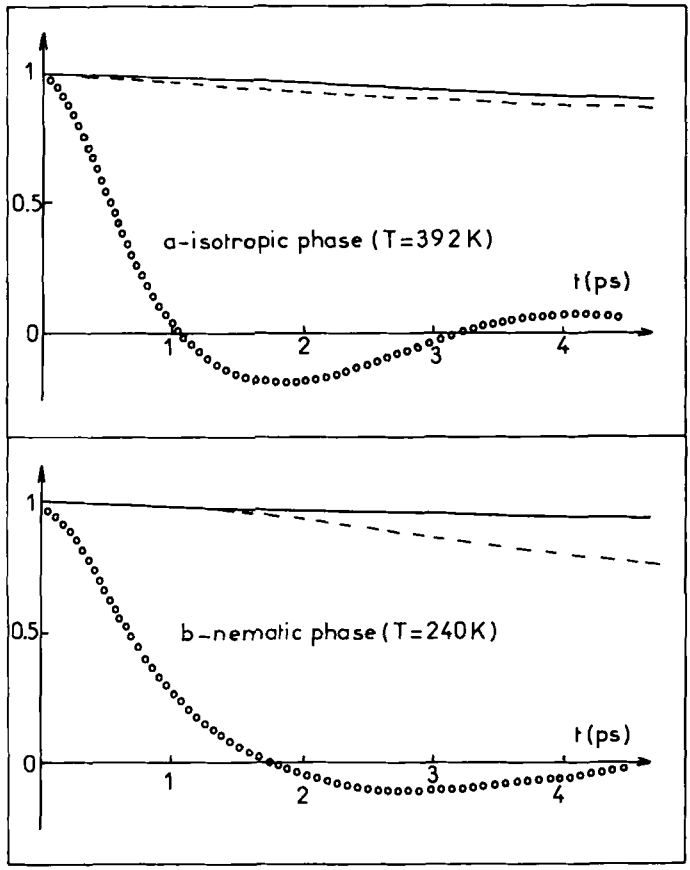

FIGURE 4 Time behavior of the parallel reorientational s.c.f. (——); the perpendicular reorientational s.c.f. (- - -); the angular momentum s.c.f. (ooo).

the two s.c.f. $\phi_{u_\parallel}$ and $\phi_{u_\perp}$ are quasi-similar. The angular momentum s.c. functions

$$\phi_J(t) = \frac{\langle J(0)J(t)\rangle}{\langle J(0)^2\rangle} \tag{10}$$

given in Figure 4 show a negative region related to the predominance of steric effects.[16] In the isotropic phase, the τ_j and τ_u relaxation times of $\phi_J(t)$ and $\phi_u(t)$, defined from

$$\tau_J = \int_0^\infty \phi_J(t)\, dt$$

and $\phi_u(t) \sim e^{-t/\tau_u}$ respectively are consistent with the Hubbard relation

$$\tau_u \cdot \tau_J = \frac{I}{2k_BT}$$

(I: moment of inertia); this means that the particles are characterized by a rotational diffusive motion.[16] In Table III we compare the critical frequencies defined as $F_c = \frac{1}{2}\pi\tau_u$ with those obtained from dielectric relaxation.[17] The calculated frequencies are higher than the experimental values.

The center of gravity velocity s.c.f.

$$\phi_{v_{\parallel'\perp}}(t) = \frac{\langle v_{\parallel'\perp}(0)v_{\parallel'\perp}(t)\rangle}{\langle v_{\parallel'\perp}(0)^2\rangle} \tag{11}$$

where $v_\parallel$ and $v_\perp$ are the components of the center of gravity velocity parallel and perpendicular to the optical axis are reported in Figure 5. The time decay of these functions in the nematic phase shows that the translational motions along the optical axis are less hindered than those in the perpendicular direction. The translational diffusion constants have been deduced from the correlation time

$$\tau_v = \int_0^\infty \phi_v(t)\,dt$$

of the velocity using

$$D = kT\tau_v/m \tag{12}$$

Some results are reported in Table IV and compared with experimental data. The calculated data are higher than the experimental values.

Qualitatively, the simulated systems are close to a nematic system. More quantitatively, we observe large statistical errors—a system which is too fluid and particles which move too easily. However, these results could be expected from the technical limits of the method, *e.g.* the small number of particles, the periodic boundaries and the two-body potential which does not take into account all of the microscopic mechanisms (dipole moments,

TABLE III

Comparison between the critical frequencies obtained from the simulation and from experiments

T	Dielectric relaxation[17]	Simulation
305.5 K	$F_{c\parallel} = 4.5$ MHz	
Nematic	$F_{c\parallel} = 100$ MHz	$F_{c\perp} = 7500$ MHz
324.5 K	$F_c = 50$ MHz	$F_c = 4000$ MHz
Isotropic		

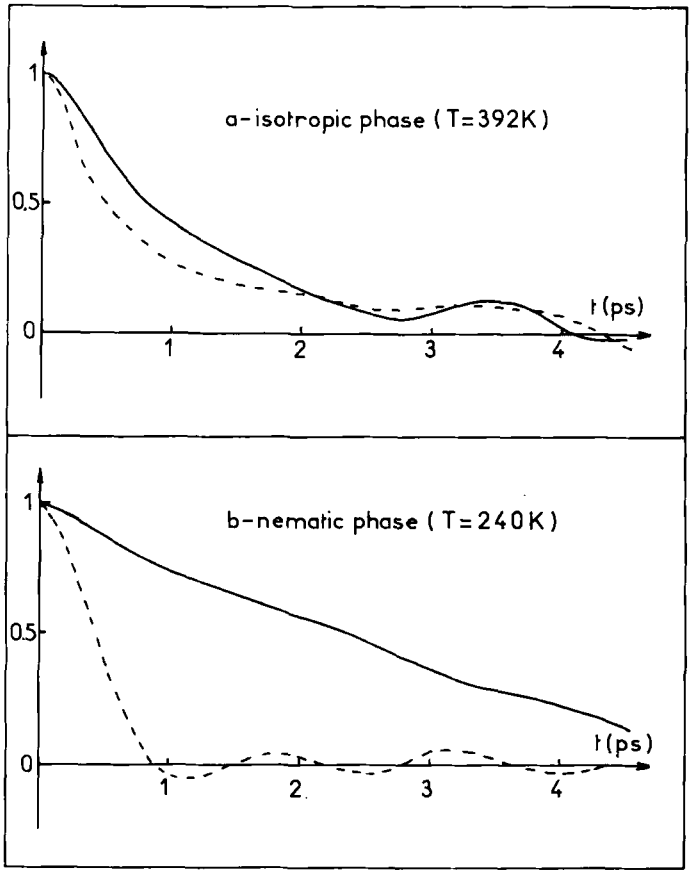

FIGURE 5 Time behavior of the center of gravity velocity s.c.f. (——) parallel and (---) perpendicular to the optical axis.

flatness of the core, long flexible tail, intramolecular movements...). Nevertheless, these first simulations give a rough picture of the physical reality and some information about the physical properties and the stability of mesophases. They can be considered as a test for the method which can be used to study other types of interaction as well.

Dipole-dipole interaction

We consider now two types of interaction: (i) the modified Lennard-Jones potential used for ellipsoidal particles and defined previously and (ii) a decentered dipole moment along the molecular axis (Figure 6), with the binary potential

TABLE IV

Comparison between the diffusion constants obtained from the simulation and from experiments

Simulation	5CB[18]	PAA[19]	TBBA[20]
$D_{\parallel} = 18$ 10^{-5} cm$^2 \cdot$ s^{-1}	$D_{\parallel} = 5.3$ 10^{-7} cm$^2 \cdot$ s^{-1}	$D_{\parallel} = 2.2$ 10^{-5} cm$^2 \cdot$ s^{-1}	$D_{\parallel} = 4$ 10^{-5} cm$^2 \cdot$ s^{-1}
$T = 300$ K	$T = 296.5$ K	$T = 397$ K	$T = 500$ K
$D_{\perp} = 4.5$ 10^{-5} cm$^2 \cdot$ s^{-1}	$D_{\perp} = 4.1$ 10^{-7} cm$^2 \cdot$ s^{-1}	$D_{\perp} = 1.2$ 10^{-5} cm$^2 \cdot$ s^{-1}	$D_{\perp} = 1.2$ 10^{-5} cm$^2 \cdot$ s^{-1}
$T = 300$ K	$T = 296.5$ K	$T = 397$ K	$T = 500$ K
$D_{\parallel}/D_{\perp} = 4$	$D_{\parallel}/D_{\perp} = 1.29$	$D_{\parallel}/D_{\perp} = 1.83$	$D_{\parallel}/D_{\perp} = 3.33$
$D_{is} = 10$ 10^{-5} cm$^2 \cdot$ s^{-1}		$D_{is} = 1.8$ 10^{-5} cm$^2 \cdot$ s^{-1}	
$T = 330$ K		$T = 416$ K	

5CB = 4-n-pentyl-4′-cyanobiphenyl.
PAA = *p*-azoxyanisole.
TBBA = Terephthalylidene-n-butylaniline.

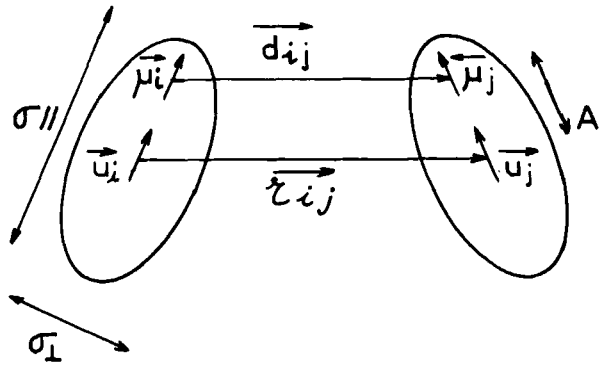

FIGURE 6 Dipole-dipole interaction: molecular shape and the decentered dipole moment.

$$W_{ij} = \frac{\mu^2}{4\pi\varepsilon_0}\left[\frac{\mathbf{u}_i \cdot \mathbf{u}_j}{d_{ij}^3} - \frac{3(\mathbf{u}_i \cdot \mathbf{d}_{ij})(\mathbf{u}_j \cdot \mathbf{d}_{ij})}{d_{ij}^5}\right] \tag{13}$$

The parameters of the model are given in Table V; they are consistent with the 7CB compound. At the beginning of the calculation, the head-to-tail molecular arrangement is required.

At $T = 300$ K, the distribution of the centers of gravity along the optical axis given by

TABLE V

Parameters of the model; the case of ellipsoidal particles with a decentered dipole moment

m (kg)	I (kg · m^2)	$\sigma_\parallel$ (Å)	$\sigma_\perp$ (Å)	ε_0/k_B (K)	μ (D)	A (Å)	N/V (m^{-3})	N
$4.61\ 10^{-25}$	$17.5\ 10^{-44}$	17.9	4.5	790	2.23	6.75	$2.16\ 10^{-27}$	8

$$g_z(z) = \frac{\langle \Delta N(z, z + \Delta z) \rangle}{N} \tag{14}$$

where ΔN is the number of centers of gravity between the planes z and $z + \Delta z$, presents two sharp peaks with a 13 Å separation (Figure 7a). This system clearly presents a partially bilayer structure[21] with a 30.9 Å layer thickness and a pair length to molecular length ratio equal to 1.73. The velocity s.c.f. (Figure 8) lead to diffusion constants (Table VI) in rather good agreement with the recent experiments of Martin *et al.*[22] on the smectic A phase of 8CB. In this case, the diffusion constants are characterized by lower values along the optical axis than those obtained for the

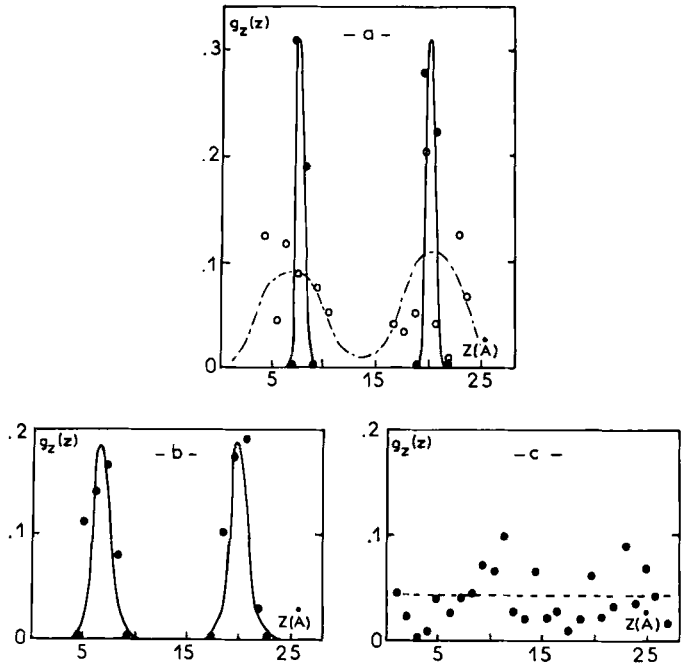

FIGURE 7 Center of gravity distribution along the optical axis: (a) (——) with dipole moment T = 300 K, (— –) without dipole moment T = 280 K; (b) with dipole moment T = 380 K; (c) with dipole moment T = 480 K.

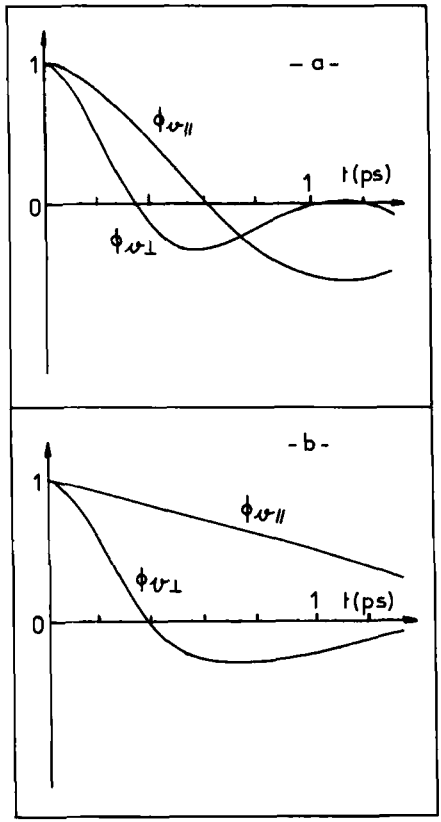

FIGURE 8 Time behavior of the center of gravity velocity s.c.f. parallel and perpendicular to the optical axis: (a) with dipole moment T = 300 K, (b) without dipole moment T = 280 K.

TABLE VI

Diffusion constants; influence of the dipole-dipole interaction and of temperature

	Dipole-dipole interaction	T	$D_{\parallel}$ ($cm^2 \cdot s^{-1}$)	$D_{\perp}$ ($cm^2 \cdot s^{-1}$)
Experiments 8CB[22]		296 K	$0.104\ 10^{-5}$	$0.134\ 10^{-5}$
Simulation	Yes	300 K	$0.07\ 10^{-5}$	$0.21\ 10^{-5}$
Simulation	Yes	380 K	$0.9\ 10^{-5}$	$1.45\ 10^{-5}$
Simulation	Yes	480 K	$1.8\ 10^{-5}$	$0.53\ 10^{-5}$
Simulation	No	280 K	$7.9\ 10^{-5}$	$0.04\ 10^{-5}$

perpendicular axis. Without dipole moment, the partially bilayer structure disappears (Figure 7a, Figure 8b, and Table VI); the system becomes nematic-like. With a dipole moment, at T = 380 K, the bilayer structure

remains (Figure 7b and Table VI) but disappears for $T = 480$ K and the system looks like a nematic (Figure 7c and Table VI). Therefore, the influence of dipole-dipole interactions and temperature on the bilayer structure of the system has been shown.

CONCLUSION

Since the method involved consists of studying a small number of particles over a short run, it can be compared with a "seed" for the "growth" of a liquid crystal. With this meaning, the numerical method can be considered as a tool to test the effect of various kinds of interaction, such as dipole moments and of disk-like particles and pear-shaped particles, on the local structure and the stability of (not only uniaxial) mesophases.

Acknowledgments

The authors would like to thank Dr. J. Prost for several comments and fruitful discussions and Mr. Y. Tinel for his technical aid.

References

1. J. Kushick and B. J. Berne, *J. Chem. Phys.*, **64**, 1382 (1976).
2. A. L. Tsykalo and A. D. Bagmet, *Mol. Cryst. Liq. Cryst.*, **46**, 111 (1978); A. L. Tsykalo, *Sov. Phys. Tech. Phys.*, **25**, 28 (1980); *Sov. Phys. Dokl (USA)*, **26**, 206 (1981).
3. J. Y. Denham, G. R. Luckhurst, C. Zanonni and J. W. Lewis, *Mol. Cryst. Liq. Cryst.*, **60**, 185 (1980); G. R. Luckhurst and S. Romano, *Mol. Phys.*, **40**, 129 (1980); see also C. Zanonni in *The Molecular Physics of Liquid Crystals* (Eds. G. R. Luckurst and G. W. Gray), Academic Press, New York, Chapter 9, 1979.
4. C. Zanonni and M. Guerra, *Mol. Phys.*, **44**, 849 (1981).
5. J. A. Barker and D. Henderson, *Rev. Mod. Phys.*, **48**, 587 (1976).
6. L. Verlet, *Phys. Rev.*, **159**, 98 (1967); **165**, 201 (1968); **A2**, 2514 (1970).
7. J. Barojas, D. Levesque and B. Quentrec, *Phys. Rev.*, **A7**, 1092 (1973).
8. B. J. Berne and P. Pechukas, *J. Chem. Phys.*, **56**, 4213 (1972).
9. H. P. Schad and M. A. Osman, *J. Chem. Phys.*, **75**, 880 (1981).
10. A. J. Leadbetter, R. M. Richardson and C. N. Colling, *J. Phys. (Paris)*, **36**, 37 (1975); A. J. Leadbetter, J. C. Frost, J. P. Gaughan, G. W. Gray and A. Mosley, *J. Phys. (Paris)*, **40**, 375 (1979).
11. D. A. Dunmur and W. H. Miller, *J. Phys. (Paris)*, **40**, 141 (1979).
12. M. Constant and D. Decoster, *J. Chem. Phys.*, **76**, 1708 (1982).
13. H. J. Coles and C. Strazielle, *Mol. Cryst. Liq. Cryst.*, **55**, 537 (1979).
14. P. G. de Gennes, *The Physics of Liquid Crystals*, Clarendon Press, Oxford (1974).
15. F. Barbarin, J. P. Chausse, C. Fabre and J. P. Germain, *J. Phys. (Paris)*, **42**, 1183 (1981).
16. R. Fauquembergue, P. Descheerder and M. Constant, *J. Phys. (Paris)*, **38**, 21 (1977); M. Constant and R. Fauquembergue, *J. Chem. Phys.*, **72**, 2459 (1980).
17. D. Lippens, J. P. Parneix and A. Chapoton, *J. Phys. (Paris)*, **38**, 1465 (1977); J. P. Parneix and A. Chapoton, *Mol. Cryst. Liq. Cryst.*, **78**, 115 (1981); J. M. Wacrenier, C. Druon and D. Lippens, *Mol. Phys.*, **43**, 97 (1981).
18. A. J. Leadbetter, F. P. Temme, A. Heidemann and W. S. Howells, *Chem. Phys. Lett.*, **34**, 363 (1975).

19. K. Otnes, R. Pynn, J. A. Janik and J. M. Janik, *Phys. Lett.*, **38A**, 335 (1972).
20. G. J. Kruger and R. Weiss, *J. Phys. (Paris)*, **38**, 357 (1977).
21. J. Prost, in *Liquid Crystals of One- and Two-Dimensional Order* (Eds. W. Helfrich and G. Heppke) Springer Series in Chemical Physics, Springer Verlag, Berlin and New York, Vol. 11, p. 125 (1980); A. M. Levelut, B. Zaghloul and F. Hardouin, *J. Phys. (Paris) Lett.*, **43**, 83 (1982) and references therein.
22. J. F. Martin, L. S. Selwyn, R. R. Vold and R. L. Vold, *J. Chem. Phys.*, **76**, 2632 (1982).